

initial electron coordinate $x_0=0.038\lambda$, $y_0=0$, and $z_0=0$, initial momentum $p_x=0$ and $p_y=0$, electron energy $\epsilon_e=60$ MeV, and undulator length $L=1$ m corresponding to 38.18λ . By numerically calculating the Hamiltonian equations, the trajectory and energy of a single electron for FW, BW and SW are shown in Fig. 2.

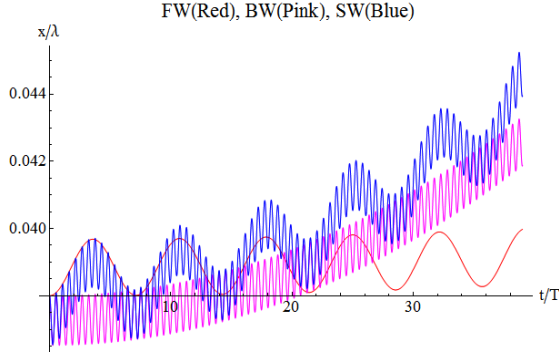


Figure 2: Transverse trajectory of single electron for FW, BW and SW ($\varphi=0^\circ$).

The numerical results shown in Fig. 2 reveal that, for FW, the motion of an electron has a low oscillation frequency $\sim(1-k_z/k)f$. For BW the oscillation frequency is high, $\sim(1+k_z/k)f$. Thus, the trajectory under SW contains multiple frequencies.

For electron beam near the waveguide axis, with beam radius $r_m \sim 1 \text{ mm} = 0.038\lambda \ll R_0 \sim \lambda$ for $f=11.424$ GHz, the Bessel function in the vector potential of Eq. (1) and (2) can be approximately expanded into a Taylor series up to the second order; thus, $J_0(k_r r) = 1 - k_r^2 r^2/4$, $J_1(k_r r) = k_r r/2 - (k_r r)^3/8$, and the dimensionless undulator field is $K = (eB_{ym}/m\omega)(1 - k_r^2 r^2/4)$. The beam radius $r_m \sim 0.038\lambda$, $k_r^2 r_m^2/4 \approx 0.004$, $r_m k_r^2/k_z = 0.07$; thus, $|A_z| \ll |A_x|$ for electrons close to the axis. Besides, when R_0 increases, k_r becomes small; thus, the transverse field becomes relative uniform. It is reasonable to take a constant K and neglect A_z as a first step, and the oscillation of longitudinal motion is determined by the transverse wiggling motion. The normalized longitudinal velocity for BW approximately can be derived as

$$\beta_{zB} = \sqrt{1 - \beta_{xB}^2 - 1/\gamma^2} \approx \left\{ 1 - \frac{1 + K^2/2}{2\gamma^2} + \frac{K^2 \cos(2(k + k_z)z)}{4\gamma^2} \right\} \quad (7)$$

The initial longitudinal velocity is $\beta_{z0} = (1 - \gamma^{-2})^{0.5}$, thus $\Delta\beta_{zB} = \beta_{zB} - \beta_{z0}$, similarly, the normalized longitudinal velocity for FW approximately yields,

$$\beta_{zF} \approx \left\{ 1 - \frac{1 + K^2/2}{2\gamma^2} + \frac{K^2 \cos(2(k - k_z)z)}{4\gamma^2} \right\} \quad (8)$$

The normalized longitudinal velocity for SW approximately can be derived as,

$$\beta_{zS} = \sqrt{1 - \beta_x^2 - 1/\gamma^2} \approx \left\{ 1 - \frac{1 + K^2}{2\gamma^2} - \frac{K^2 (-\cos(2kz) + \cos(2k_z z))}{2\gamma^2} \right. \\ \left. - K^2 (\cos(2(k + k_z)z) + \cos(2(k - k_z)z)) / (4\gamma^2) \right\} \quad (9)$$

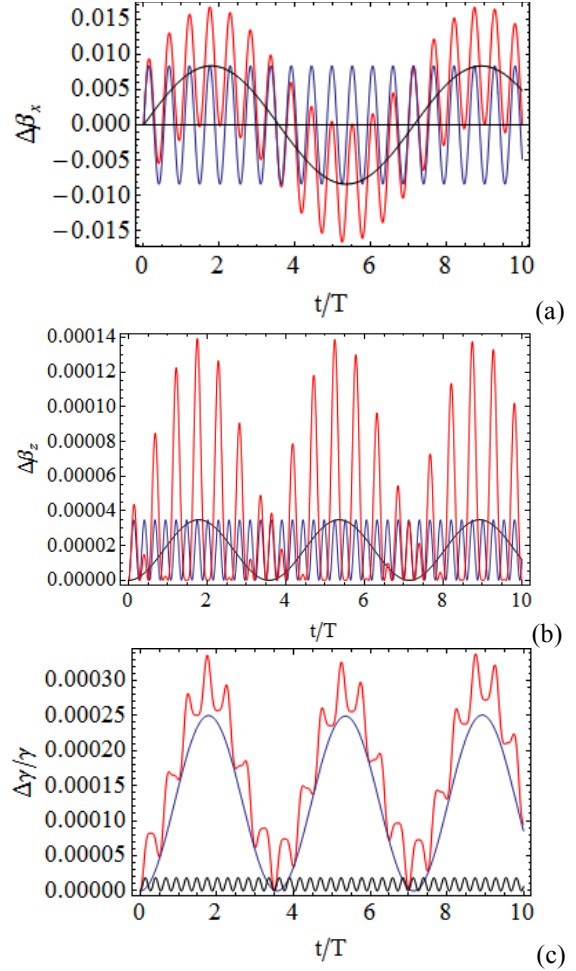


Figure 3: Comparison of numerical (a) $\Delta\beta_x$, (b) $\Delta\beta_z$, and (c) $\Delta\gamma/\gamma$ for BW (blue), FW (black), and SW (red) with $A_z=0$. ($K=1$, $\gamma=117.4$).

If $A_z=0$, electrons at different transverse positions, from the axis to $x_m = \pm 0.038\lambda$, have the same amplitude of $\Delta\beta_x$, $\Delta\beta_z$ and $\Delta\gamma/\gamma$ no matter for BW, FW, or SW, since $J_0(k_r r) = 1 - k_r^2 r^2/4$ changes little. Comparisons of numerical $\Delta\beta_x$, $\Delta\beta_z$, and $\Delta\gamma/\gamma$ for BW, FW, and SW are shown in Fig. 3. It is found that the analytical values of $\Delta\beta_z$ for BW, FW, and SW from Eqs. (7-9) are perfectly consistent with the numerical ones in Fig. 3(b). Note that the longitudinal motion contains four harmonic oscillations for SW. The energy spread $\Delta\gamma/\gamma$ for SW mainly arises from FW and reaches about 0.03% for $\epsilon_e=60$ MeV.

After considering A_z , electrons at different transverse positions have significantly different amplitudes of $\Delta\gamma$, which increases to 0.4% at $x_m = \pm 0.038\lambda$ ($\sim \pm 1$ mm), significantly larger than that on the axis, since $A_z \sim J_1(k_z r)$ quickly increases. $\Delta\gamma/\gamma$ for SW mainly arises from the influence of A_z of FW, shown in Fig. 4. Decreasing the beam size in both transverse directions has a better effect on diminishing energy spread in an RF undulator.

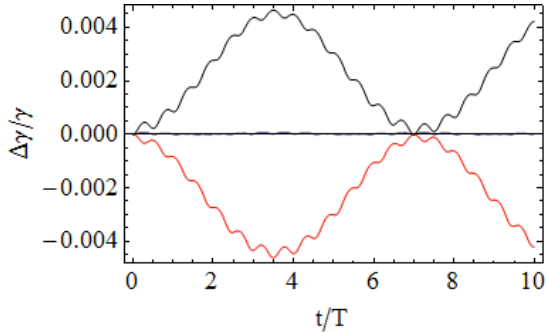


Figure 4. Variation of $\Delta\gamma/\gamma$ for SW with A_z , where $x=0$ (blue), $x=x_m \sim 0.038\lambda$ (black), $x=-x_m$ (red) ($K=1$, $\gamma=117.4$).

CONCLUSION

The forward and backward wave (FW/BW) components have different contributions to electron motion and radiation. For FW, the motion of electron has a low oscillation frequency $\sim(1-k_z/k)f$. As a comparison, for BW, a high oscillation frequency $\sim(1+k_z/k)f$. Thus, trajectory under SW contains multiple frequencies. Most of the energy spread comes from the FW component; the effect of FW on modulating the electron energy is much stronger than that of BW for the same undulating-amplitude value.

REFERENCES

- [1] Shea, F., Marcus, G. Rosenzweig, J. B., Scheer, M. Bahrtdt, J., Weingartner, R., Gaupp, A. Gruner, F., "Short Period, High Field Cryogenic Undulator for Extreme Performance X-ray Free Electron Lasers," *Phys. Rev. ST Accel. Beams* **13** (2010) 070702.
- [2] S. Tantawi, V. Dolgashev, C. Nantista, C. Pellegrini, J. Rosenzweig, G. Travish, "A Coherent Compton Backscattering High Gain FEL using an X-Band Microwave Undulator," 2005 FEL Conference, Stanford, California, USA; <http://accelconf.web.cern.ch/accelconf/f05/PAPERS/THOA006.PDF>
- [3] T. Shintake, K. Huke, J. Tanaka, I. Sato and I. Kumabe, "Development of microwave undulator", *Japanese J. of Appl. Phys.* **22** (1983), p. 844-851.
- [4] T.M. Tran, B.G. Danly, J.S. Wurtele, "Free-Electron Lasers with Electromagnetic Standing Wave Wigglers", *IEEE J. Quantum Electronics* **QE-23** (1987), pp. 1578-1589.
- [5] M. Yeddulla, H. Geng, Z. Ma, Z. Huang, S. Tantawi, "Waveguide Structures for RF Undulators with Applications to FELs and Storage Rings," *Proceedings of EPAC08, Genoa, Italy*; <http://accelconf.web.cern.ch/accelconf/e08/papers/wepc136.pdf>
- [6] C. Pellegrini, "X-Band Microwave Undulators for Short Wavelength Free-Electron Lasers," 2005 FEL Conference 2005, Stanford, California, USA; <http://accelconf.web.cern.ch/accelconf/f05/PAPERS/MOPP060.PDF>
- [7] P.J.B. Clarricoats and A.D. Olver, *Corrugated horns for microwave antennas*, Peter Peregrinus Ltd, London, UK, 1984.